On the seasonal onset of polar mesospheric clouds and the breakdown of the stratospheric polar vortex in the Southern Hemisphere

B. Karlsson,[1] C. E. Randall,[1,2] T. G. Shepherd,[3] V. L. Harvey,[1] J. Lumpe,[4] K. Nielsen,[4] S. M. Bailey,[5] M. Hervig,[6] and J. M. Russell III[7]

Received 23 March 2011; revised 15 June 2011; accepted 21 June 2011; published 22 September 2011.

[1] Southern Hemisphere (SH) polar mesospheric clouds (PMCs), also known as noctilucent clouds, have been observed to be more variable and, in general, dimmer than their Northern Hemisphere (NH) counterparts. The precise cause of these hemispheric differences is not well understood. This paper focuses on one aspect of the hemispheric differences: the timing of the PMC season onset. Observations from the Aeronomy of Ice in the Mesosphere satellite indicate that in recent years the date on which the PMC season begins varies much more in the SH than in the NH. Using the Canadian Middle Atmosphere Model, we show that the generation of sufficiently low temperatures necessary for cloud formation in the SH summer polar mesosphere is perturbed by year-to-year variations in the timing of the late-spring breakdown of the SH stratospheric polar vortex. These stratospheric variations, which persist until the end of December, influence the propagation of gravity waves up to the mesosphere. This adds a stratospheric control to the temperatures in the polar mesopause region during early summer, which causes the onset of PMCs to vary from one year to another. This effect is much stronger in the SH than in the NH because the breakdown of the polar vortex occurs much later in the SH, closer in time to the PMC season.

Citation: Karlsson, B., C. E. Randall, T. G. Shepherd, V. L. Harvey, J. Lumpe, K. Nielsen, S. M. Bailey, M. Hervig, and J. M. Russell III (2011), On the seasonal onset of polar mesospheric clouds and the breakdown of the stratospheric polar vortex in the Southern Hemisphere, *J. Geophys. Res.*, *116*, D18107, doi:10.1029/2011JD015989.

1. Introduction

[2] Polar Mesospheric Clouds (PMCs) exist in the high latitude mesopause region between late November and mid February in the Southern Hemisphere (SH), and between late May and late August in the Northern Hemisphere (NH), i.e., sometime between day −40 and day 90 relative to the summer solstice. During this period, the polar mesopause region is the coldest place in Earth's atmosphere. The low temperatures necessary for these clouds to form are linked to the meridional circulation of the mesosphere, which in the summer hemisphere is directed toward the equator. By mass continuity, upwelling occurs at high latitudes, and the ascending air is cooled adiabatically to temperatures lower than 150 K [e.g., *Lübken*, 1999]. In addition to lowering the temperatures, this upward flow transports water vapor to the summer polar mesopause region, and also causes PMCs, that are mostly composed of water ice [*Hervig et al.*, 2001], to remain in the super saturated altitude range longer so that they can grow larger. Because all three effects act in the same direction, PMCs are excellent indicators of the strength of the mesospheric upwelling above the summer pole. Since super saturation is exponentially dependent on temperature and only linearly dependent on water vapor, the clouds are primarily controlled by temperature [e.g., *Hervig et al.*, 2009]. In the winter hemisphere, the circulation is instead directed toward the pole, where the air descends and warms adiabatically at high latitudes. This summer-to-winter mesospheric flow is driven by gravity waves (GWs). These waves propagate upwards, primarily from sources in the troposphere, and break at high altitudes, depositing their momentum into the background flow [*Lindzen*, 1981], which on average is primarily zonal. The momentum deposition causes a so-called 'drag' on the (zonal) flow. This gravity wave drag (GWD) can have either a decelerating or an accelerating effect, depending on the sign of the waves' intrinsic phase speed. Changes in the zonal flow due to the GWD

[1]Laboratory for Atmospheric and Space Physics, University of Colorado at Boulder, Boulder, Colorado, USA.
[2]Department of Atmospheric and Oceanic Sciences, University of Colorado at Boulder, Boulder, Colorado, USA.
[3]Department of Physics, University of Toronto, Toronto, Ontario, Canada.
[4]Computational Physics, Inc., Boulder, Colorado, USA.
[5]Bradley Department of Electrical and Computer Engineering, Virginia Polytechnic Institute and State University, Blacksburg, Virginia, USA.
[6]GATS, Inc., Driggs, Idaho, USA.
[7]Center for Atmospheric Sciences, Hampton University, Hampton, Virginia, USA.

0148-0227/11/2011JD015989

immediately distort the mass-wind balance. To regain the balance, a meridional circulation is induced [see, e.g., *Shepherd*, 2000].

[3] Whereas GWs affect the zonal flow, the opposite is also true. While propagating through the atmosphere, GWs are filtered by the background zonal wind through critical-layer absorption [see, e.g., *McLandress*, 1998]. In the summer hemisphere, heating from absorption of solar radiation maximizes at high latitudes, leading to a temperature gradient that points toward the pole throughout the stratosphere; via thermal wind balance this gives rise to easterly (westward) winds in the middle atmosphere, overlaying the westerly (eastward) winds in the upper troposphere. Consequently, only gravity waves with sufficiently large eastward phase speeds (i.e., larger than the maximum upper tropospheric winds) can propagate through the summer middle atmosphere, where they exert a positive drag on account of their eastward intrinsic phase speeds. In the winter hemisphere, the temperature gradient is reversed and the stratospheric winds are westerly. Thus the eastward propagating gravity waves are filtered out in the stratosphere, while westward propagating and stationary (i.e., orographic) gravity waves can reach the mesosphere, where they exert a negative drag on account of their eastward intrinsic phase speeds. The opposite signs of the momentum deposition from the breaking of the oppositely directed gravity waves explain the different direction (with respect to the pole) of the meridional flow between the summer and the winter hemisphere (see, e.g., *Shepherd* [2000]).

[4] The transition between winter and summer zonal winds in the mesosphere usually occurs in late March to early April in the NH, and in mid-October in the SH [*Dowdy et al.*, 2007]. The timing of this shift is to first order controlled by the reappearance of sunlight at high latitudes, which causes the polar upper stratosphere (the region of maximum ozone heating) to warm, changing the equator-to-pole temperature gradient and thereby the zonal winds in the mesosphere above. In the lower stratosphere, however, ozone heating is much weaker and the breakdown of the polar westerlies is induced by dynamical heating from breaking planetary waves, in the so-called "final warming." This means that the timing of the lower-stratospheric breakdown can vary from year to year, as a result of natural variability in the wave forcing. In the SH, the weaker planetary wave forcing compared with the NH causes the lower stratospheric vortex breakdown to be considerably delayed relative to the NH, so that this variability in vortex breakdown can influence stratospheric conditions in early summer [*Waugh et al.*, 1999; *Black and McDaniel*, 2007]. Because the zonal flow affects GW propagation, interannual variations in the timing of the lower stratospheric wind reversal will cause interannual variations in the GW-driven meridional circulation, and thus temperature, in the PMC region. Therefore, changes in the timing of the winter-to-summer stratospheric wind reversal could in principle explain the observed differences in the onset date of the SH PMC seasons. We investigate this hypothesis in this paper.

[5] In section 2, we describe the data sources used in this study. Observations of PMCs along with the conditions in the lower atmosphere are shown in Section 3, and in Section 4 the mechanism is demonstrated using model simulations. The results are discussed in Section 5.

2. Data

[6] Data used for this study come from satellite observations, a meteorological reanalysis, and a free-running, comprehensive general circulation model. The Aeronomy of Ice in the Mesosphere (AIM) satellite, launched in 2007, is the first space-based experiment that is solely dedicated to observing PMCs [*Russell et al.*, 2009]. Two of the three instruments onboard the spacecraft are used in this study. Among other parameters, the Solar Occultation For Ice Experiment (SOFIE) measures temperature and ice extinction profiles using eleven wavelengths from 0.330 to 5.10 μm with a vertical resolution of 1–2 km [e.g., *Gordley et al.*, 2009; *Hervig et al.*, 2009]. The Cloud Imaging and Particle Size instrument (CIPS) measures the sunlight scattered by the clouds at a wavelength of 265 nm [*Bailey et al.*, 2009; *Rusch et al.*, 2009]. The instrument consists of four nadir-viewing cameras that together cover an area of approximately 2000 × 1000 km in the polar region, with a horizontal resolution in the nadir of ~2 km [*McClintock et al.*, 2009]. CIPS data quality was evaluated by *Benze et al.* [2009]. Here, we use CIPS to get PMC frequency of occurrence.

[7] December zonal mean zonal wind and zonal mean temperature data from the European Centre for Medium Range Weather Forecasts Interim Re-Analysis (ECMWF ERA-Interim) are used to characterize the state of the lower atmosphere (1000 to 1 hPa) during the onset of three cloud seasons in the SH. For more information about the ERA-Interim product, see *Simmons et al.* [2007].

[8] The extended version of the Canadian Middle Atmosphere Model (CMAM) [*Fomichev et al.*, 2002; *McLandress et al.*, 2006] covers the atmosphere from Earth's surface up to approximately 210 km. Its vertical and horizontal resolution is approximately 3 km (in the mesosphere) and 6°, respectively. All relevant physical processes in the middle atmosphere are included in CMAM, as described by *Fomichev et al.* [2002]. The non-orographic gravity waves are parameterized using the parameterization scheme of *Hines* [1997a, 1997b]; note that orographic waves can play no role in the summertime mesosphere, because they are filtered by the zero-wind line in the lower stratosphere.

3. The Onset of the SH PMC Season and Its Relationship to the Lower Atmosphere

[9] Figure 1 illustrates PMC observations by AIM from a total of 7 seasons. The thick lines in Figure 1 denote observations from the SH (November to February), the focus of this study. The thin black lines are NH observations from 2007 to 2010 (May to August) and are included for comparison. The PMC occurrence frequencies at latitudes >50° observed by the CIPS instrument on AIM are shown in Figure 1a. It is obvious from this figure that the seasonal onset of clouds in the SH varies considerably more than in the NH. In the SH seasons 07/08 and 08/09, the clouds formed later relative to solstice than in the NH. However, in SH 09/10, the clouds formed earlier than in any other season (in either hemisphere) observed by AIM.

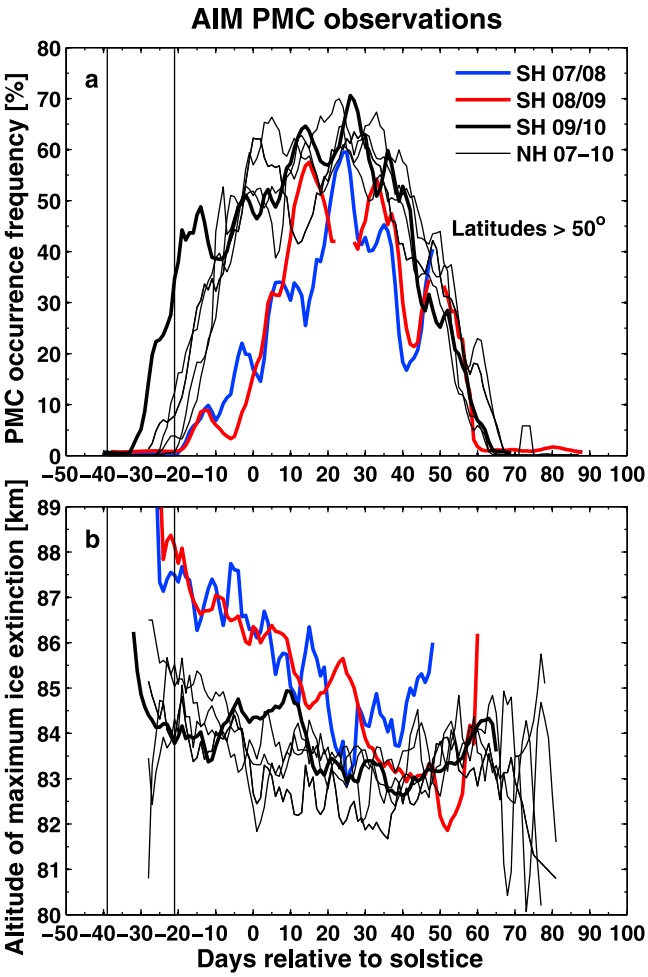

Figure 1. (a) CIPS PMC occurrence frequencies poleward of 50° latitude, and (b) altitude of maximum ice extinction observed by SOFIE. The thick curves show the SH seasons, labeled by year, and the thin black curves indicate observations from the NH. Thin vertical lines denote the PMC "onset period" (see text for details).

[10] In Figure 1b, the altitude of maximum ice extinction at 3.064 μm observed by the SOFIE instrument on AIM is shown. The 07/08 and 08/09 SH clouds are higher in altitude than in 09/10. In fact, cloud altitudes in the 09/10 season are more similar to those in the NH seasons than to other SH seasons. The altitude difference is largest in the early part of the season.

[11] To investigate the atmospheric conditions that are responsible for the differences in the seasonal onset of the SH clouds in 2009 compared to 2007 and 2008, we now focus on the second half of November (day −40 to day −20, denoted by the vertical lines). As described above, the low temperatures required for PMC formation in the summer polar mesopause region are attributed to deposition of positive momentum from breaking GWs. Since the zonal wind in the lower stratosphere determines which part of the GW spectrum can propagate vertically at this time of year, modulation of this flow will affect the GWD in the mesosphere. Figure 2 shows the zonal mean zonal wind (U) at 50 hPa and 65°S. Here it can be seen that in late November (denoted by the vertical lines), and in December (day −20 to day 10), the zonal mean westerlies in the 07/08 and 08/09 seasons are stronger than in the 09/10 season. That is, the stratospheric winds shifted to more summer-like conditions earlier in the 09/10 season than in the 07/08 or 08/09 seasons. Since this shift changes the GW filtering, which controls the temperature of the summer polar mesopause, this could explain why SH PMCs formed earlier in the 09/10 season than in the other two seasons. Consistent with this explanation, the mesopause temperature measured by SOFIE (not shown) decreased earlier in the 09/10 season than in the other AIM seasons. The gray curve and the shading in Figure 2 denote the ERA-Interim 21-year mean and the one standard deviation about the mean, respectively. In 2009, the zonal mean wind is close to climatology. This indicates that the PMC onsets in 2007 and 2008 (see Figure 1) are unusually late, rather than the onset in 2009 being unusually early.

[12] Figure 3 shows the ERA-Interim zonal mean zonal wind anomaly (ΔU) and the zonal mean temperature anomaly (ΔT) averaged between day −40 and day −20 relative to solstice. This time frame will be referred to as the "onset period," for simplicity, even though, as can be seen in Figure 2, the differences in stratospheric conditions persist until about day 20. The anomaly fields are created by removing the 21-year ERA-Interim mean of wind and temperature from the year and period of interest. Anomalies exceeding one standard deviation (std) of the ERA-Interim wind and temperature fields are contoured in black dashed lines. The ERA-Interim data reach up to 1 hPa. As an indication of the region where the clouds form, the polar summer mesopause region is denoted by the thick black 150 K contour from CMAM. It is the atmosphere in and underneath this region that is investigated in the present study. Possible influences from the variability in the winter

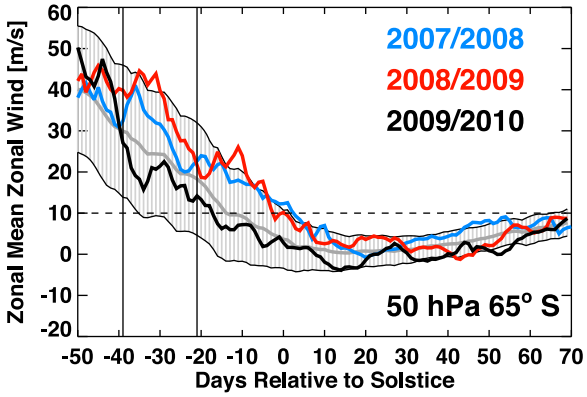

Figure 2. Zonal mean zonal wind from ERA-Interim indicating the breakdown of the stratospheric polar vortex. This breakdown is defined to occur when the zonal mean wind at 50 hPa and 65°S decreases below 10 m/s (dashed line). The vertical lines denote the period of main interest for this study. The gray curve is the 21-year ERA-Interim mean and the shaded region denotes one standard deviation about the mean.

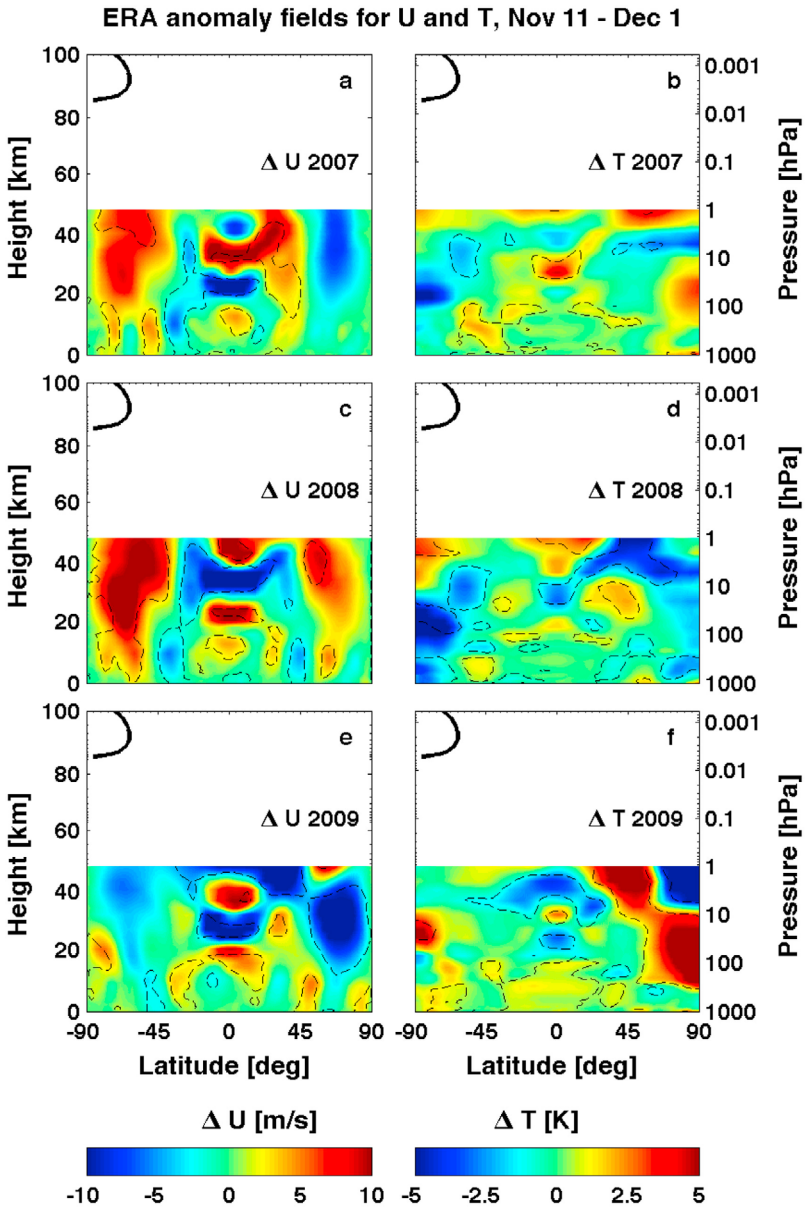

Figure 3. (a, c, and e) Wind and (b, d, and f) temperature anomaly fields from ERA-Interim for the onset period (day −40 to −20 relative to solstice) in 2007, 2008, and 2009. The thick black contour shows the location of the summer polar mesopause (from CMAM). Thin dashed curves show areas where the anomalies exceed one standard deviation.

hemisphere due to inter-hemispheric coupling, described by, e.g., *Becker and Schmitz* [2003] and *Karlsson et al.* [2009a, 2009b], are briefly discussed in Section 5.

[13] As seen in Figures 3a, 3c, and 3e, mean winds in the SH during the onset period are anomalously eastward (positive) in 2007 and 2008, whereas in 2009, the SH wind has a weak westward anomaly (negative). These wind anomalies are associated with the anomalies seen in the temperature fields (Figures 3b, 3d, and 3f). In 2007 and 2008, the anomalously low temperatures in the polar region at about 100 hPa represent a delayed breakdown of the SH winter vortex, so that the 'winter-like' conditions linger well into the SH summer.

[14] The anomaly fields for December (day −20 to day 10 relative to solstice) are illustrated in Figure 4; the interannual variability in the vortex breakdown is also evident in this month. The December anomalies are coherent with those in the onset period (Figure 3), and are consistent with the interannual differences in the PMC occurrence frequencies for December (Figure 1).

[15] As previously mentioned, we hypothesize that it is the difference in the zonal flow in the lower stratosphere that explains the observed differences in the onset of the PMC season and the higher occurrence of clouds in December 2009 as compared with the two previous years, through filtering of the GW fluxes, which affects the GWD-induced

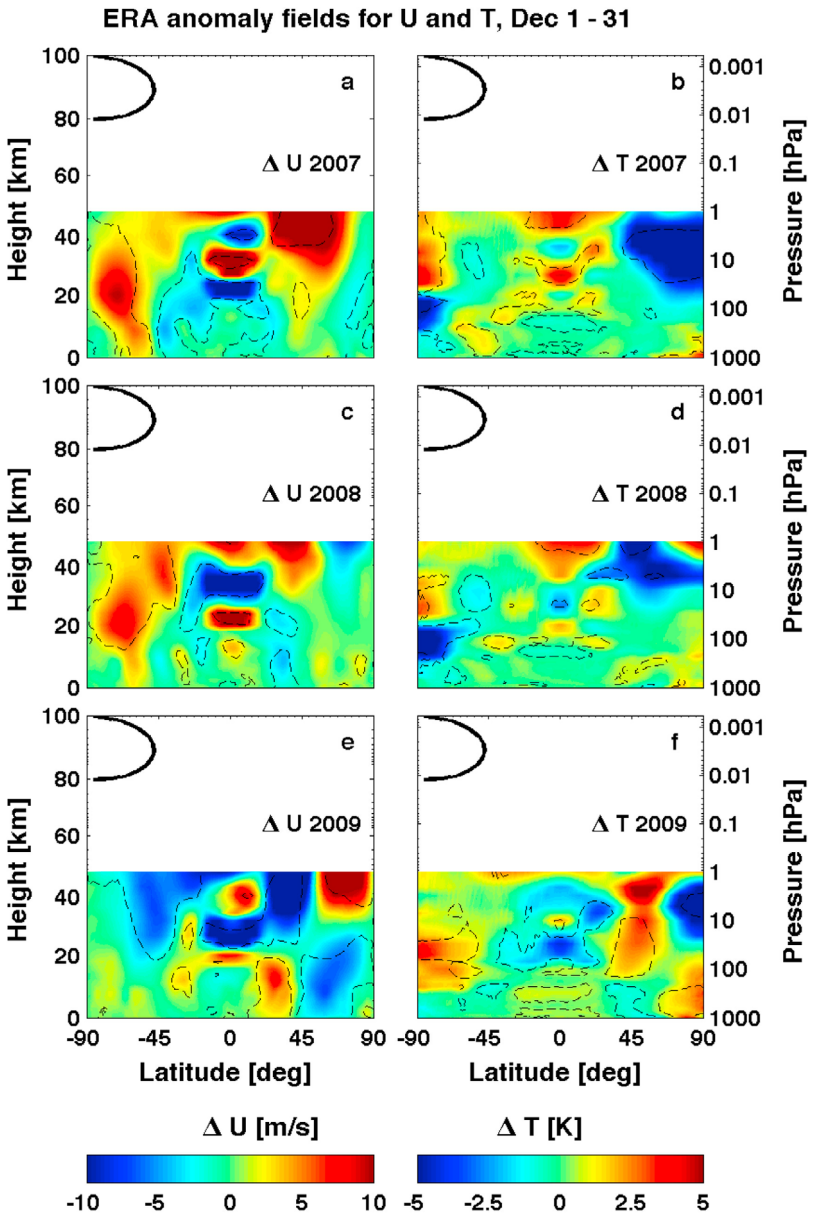

Figure 4. Same as Figure 3, but for the month of December.

meridional flow and temperature anomalies at higher altitudes. This hypothesis is investigated in Section 4.

4. Mechanism

[16] To study the conditions associated with the onset of the PMC season in the SH, we use a 19-year run of the extended CMAM. A composite study based on wind variability in the summer stratosphere at 63.7°S and 52 hPa (the model grid point closest to the location of the polar vortex breakdown criterion defined by *Langematz and Kunze* [2008]) was carried out for the onset-period (i.e., day −40 to day −20 relative to solstice) mean CMAM data. Anomalously 'summer-like' winds (early breakdown), defined as wind anomaly $\leq -0.5 \cdot$ std, where std is the standard deviation of the wind at this location and time period, as well as anomalously 'winter-like' (late breakdown) winds defined as winds $\geq 0.5 \cdot$ std, were collected from the data sets, and compared to each other. Using the threshold of $0.5 \cdot$ std, six events of both anomalously positive and anomalously negative winds were found. The mean wind and temperature anomalies of the positive and negative composites are shown in Figures 5a–5d, respectively. Only anomalies that are significant at the 95% confidence level are included in this figure. The significance is determined based on randomly generated composite means where six onset-periods were picked out 2000 times.

[17] We first note that the CMAM zonal wind and temperature fields in the SH high-latitude stratosphere for the late-breakdown anomalies (Figures 5a and 5b) are very similar to those in ERA-Interim for 2007 and 2008 (Figures 3a–3d), which are also years with late-breakdown anomalies (Figure 2). This lends credence to the use of CMAM for this study. The same comparison cannot be

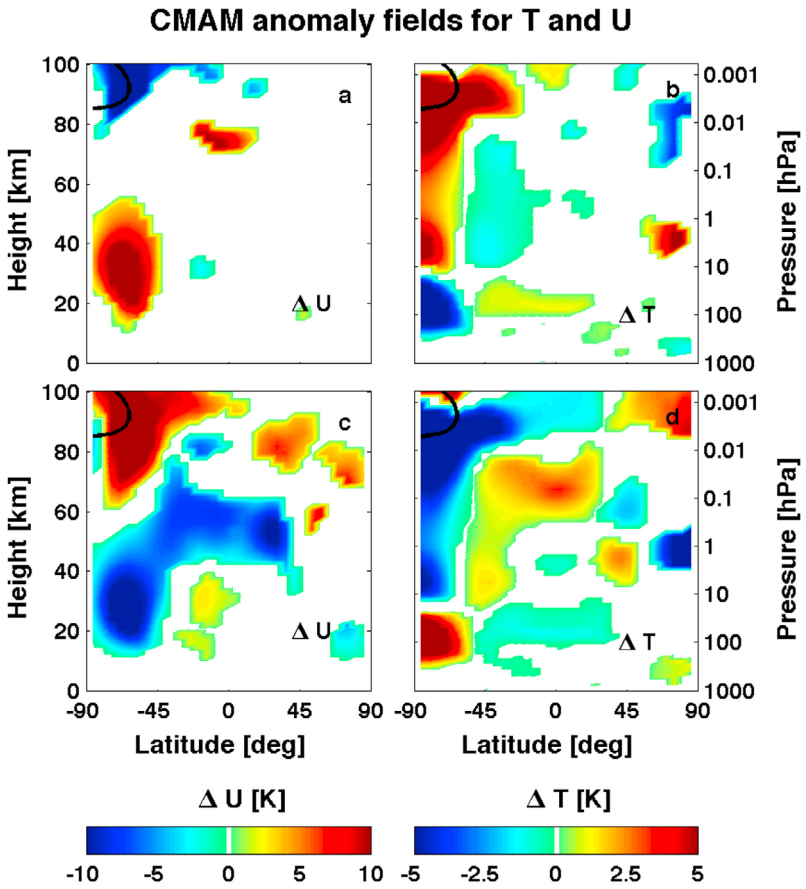

Figure 5. (a and c) Anomalous wind and (b and d) anomalous temperature responses during the onset period (day −40 to −20 relative to solstice) to a late vortex breakdown (Figures 5a and 5b) and an early vortex breakdown (Figures 5c and 5d) in CMAM.

made between the CMAM early breakdown anomalies (Figures 5c and 5d) and ERA-Interim in 2009 (Figures 3e and 3f), since 2009 was close to climatology (Figure 2).

[18] Comparing the early breakdown and late-breakdown anomaly fields in CMAM, the higher temperatures in the polar summer mesopause region (Figure 5b) associated with the late vortex breakdown could explain the absence (or lower occurrence) of PMCs during the onset period, since these are, as mentioned previously, highly sensitive to changes in temperature [*Hervig et al.*, 2009]. Conversely, when the vortex breaks down early, the high latitude mesopause is colder (Figure 5d), which would lead to an earlier seasonal onset of the clouds.

[19] The anomaly field can be explained further by considering Figure 6. Here, the CMAM profiles of zonal wind, temperature, total (net eastward plus net westward) gravity wave drag (GWD), and meridional and vertical residual velocity ($\overline{v}^*$ and $\overline{w}^*$) averaged between 55° and 75°S for the two composite groups are shown. It can be seen that the zonal mean wind maximum in the lower stratosphere is weaker for the case in which the vortex breaks down early (gray curves) than for the case of a delayed breakdown (Figure 6a), as expected. The weaker westerly maximum filters out fewer eastward propagating waves, leading to stronger GWD in the mesosphere (Figure 6c). The stronger mesospheric GWD results in an enhanced meridional flow (Figure 6e) and more polar upwelling (Figure 6f) and thus cooling (Figure 6b), which explains the anomalously cold high-latitude stratosphere and mesosphere in Figure 5d. This in turn leads to a weakening of the negative vertical wind shear throughout the mesosphere, which weakens the summertime easterlies (Figure 6a). Conversely, for the case of a late vortex breakdown (black curves), the mesospheric net GWD is weaker due to greater filtering of eastward propagating GWs reaching higher altitudes.

[20] The mechanism described above is analogous to the mesospheric response during stratospheric sudden warmings, which results from GW critical-level filtering [*Holton*, 1983]. This study shows that the same wave–mean flow interaction, arising from a relatively small change in the late-spring/early summer lower stratospheric zonal flow, is crucial for modulating the seasonal onset of PMC formation. We consider these results to be robust, since the basic mechanism of GW filtering is a well established physical phenomenon that is included in every GWD parameterization, and is not sensitive to model details. The GW morphology assumed in the model can affect the magnitude of the response, and details of its vertical structure, but cannot change its sign. Since the comparison here is only qualitative (i.e., the sign of the correlation between stratospheric winds and mesospheric temperatures), these details are insignificant for the conclusions drawn here.

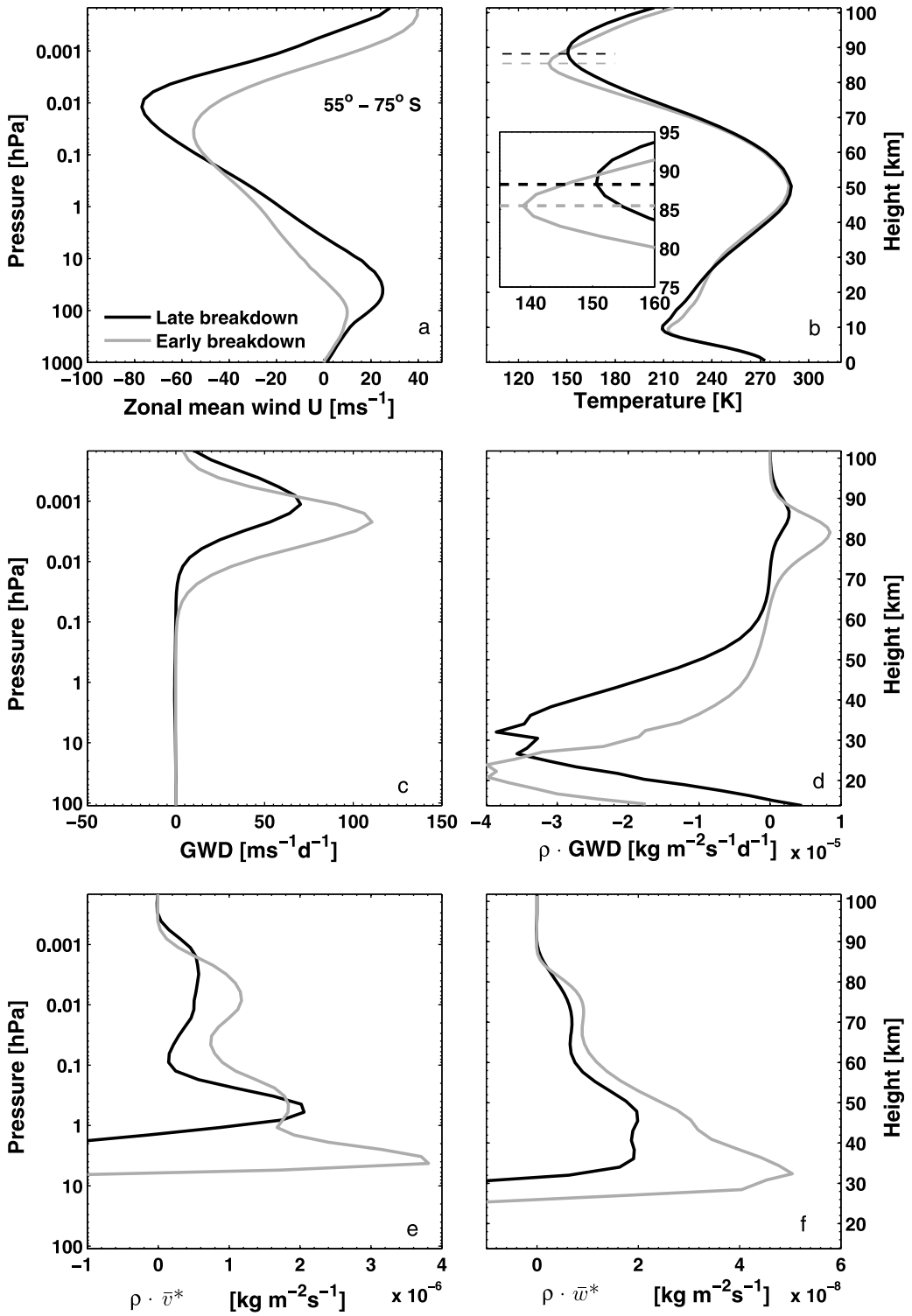

Figure 6. Zonal mean (a) wind, (b) temperature, (c) gravity-wave drag (GWD), (d) density weighted GWD, (e) density weighted meridional residual flow, and (f) density weighted vertical residual flow during the onset period for the average of the early (gray curves) and late vortex breakdowns (black curves). The profiles are averaged between 55° and 75° latitude.

[21] It should be pointed out that basically all the GWs with westward intrinsic phase speeds are filtered out below 60 km in the Hines gravity wave parameterization in the summer extratropics. In the case of an early vortex breakdown, the westward GWs have smaller intrinsic phase speeds due to the weaker zonal flow, and thus reach their breaking level lower down in the stratosphere (Figure 6d).

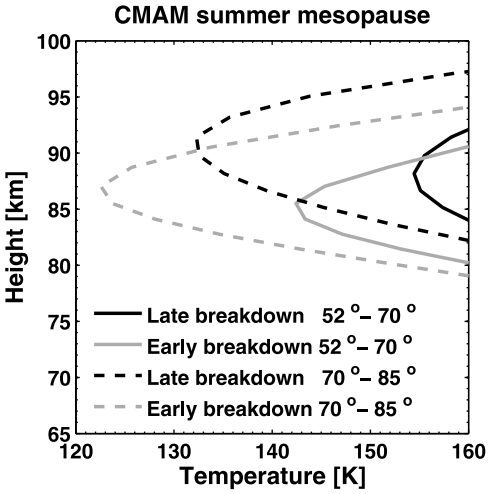

Figure 7. CMAM temperature profiles in the vicinity of the mesopause during the onset period, averaged from 52°–70°S (solid curves) and 70°–85°S (dashed curves), for the average of the early (gray curves) and late vortex breakdowns (black curves).

[22] In the mesosphere, the weakening of the easterly jet in the early breakdown case leads to smaller intrinsic phase speeds for the eastward propagating GWs, and thus their breaking levels are also shifted downward (Figures 6c and 6d). This downward shift in breaking levels leads to the differences in mesopause altitudes (~2.7 km) between a late and an early vortex breakdown, as seen in Figure 6b and in the PMC observations (Figure 1b). The CMAM mesopause is about 11 K colder during the onset period in the case of an early breakdown compared to a late breakdown.

[23] The temperature results of the CMAM analysis can now be compared to the thermodynamic conditions required for PMC formation. Although homogeneous PMC formation may take place at extreme temperatures in the summer polar mesopause [e.g., *Murray and Jensen*, 2010], condensation nuclei are in general a necessity. Smoke particles originating from meteorites are suggested to be the primary candidate for mesospheric ice nucleation sites [see *Rapp and Thomas*, 2006]. Assuming smoke particles with a radius of about 1 nm [*Gumbel and Megner*, 2009], the temperature typically has to be ~130 K in order to reach the super saturation required for cloud particles to form [*Rapp and Thomas*, 2006; *Gumbel and Megner*, 2009]. In addition, at temperatures higher than about 150 K, the cloud particles quickly sublimate. Figure 7 shows the mesopause temperature from CMAM averaged over two different latitude bands during the onset period. Considering the approximate temperature thresholds discussed above, Figure 7 shows that clouds are not likely to exist in the lower latitude band during the onset period when the breakdown of the stratospheric vortex is delayed (solid black curve). Neither would cloud nucleation occur at the higher latitude band (dashed black curve). When the stratospheric vortex breaks down earlier, however, nucleation can occur at the higher latitudes (dashed gray curve) and clouds can be sustained at lower latitudes (solid gray curve). This result strongly supports the hypothesis that the timing of the SH vortex breakdown influences the seasonal onset of PMCs.

5. Discussion

[24] We have investigated variations in the start of the PMC seasons in the SH and found strong evidence that the timing of the late-spring breakdown of the stratospheric polar vortex plays an important role in the seasonal onset of the clouds. Due to the comparative weakness of dynamical heating from planetary-wave drag as compared with the NH, the SH stratospheric polar vortex can in certain years persist well into summer, delaying the transition from westerly to easterly winds in the lower stratosphere. The westerly winds prevent a portion of the eastward propagating GW spectrum from reaching the upper stratosphere and mesosphere, thereby reducing the (positive) GWD in the mesosphere. This drag gives rise to the meridional residual flow, which drives the extremely low temperatures in the summer polar mesopause region necessary for PMCs to exist. Thus, as the drag is reduced, the meridional circulation is weakened, leaving the late-spring/early summer polar mesopause warmer than usual during years when the SH stratospheric polar vortex breakdown is late.

[25] Due to the stronger planetary-wave forcing in the NH, the NH winter vortex generally breaks down earlier (relative to solstice) than in the SH. Therefore when PMCs start forming in the NH, the summer stratospheric easterlies are already well developed and stratospheric variability is much reduced compared to the SH. The onset of NH PMCs is thus not affected by the seasonal westerly to easterly transition in the same way as in the SH (Figure 1). These differences between the stratospheric polar vortex variability in the NH and SH will naturally contribute to the hemispheric characteristics of the clouds. As discussed by *Siskind et al.* [2003], hemispheric asymmetries in the strength of the winds in the lower stratosphere may contribute to differences between NH and SH PMCs, through the same mechanism described here. If the SH vortex breakdown period persists into the summer, this would coincide with generally more winter-like stratospheric winds – synonymous with "weaker" summer winds. This could help explain why SH PMCs are in general dimmer than in the NH, at least during the time period of the vortex breakdown. Other suggested reasons for NH-SH differences in PMCs include Earth's orbital eccentricity [*Chu et al.*, 2003] and inter-hemispheric coupling [*Becker and Schmitz*, 2003; *Karlsson et al.*, 2007, 2009a].

[26] This study indicates that year-to-year variability in the seasonal onset of SH PMCs is affected by changes in the stratospheric zonal flow underneath the clouds. While the variation in cloud onset from one year to another is restricted to the period between late November and (mid) December, the differences persist through the rest of December (Figure 1) because the differences in stratospheric winds between early onset and late-onset years persist to the end of December (Figure 2) as a result of the long radiative timescale in the lower stratosphere. In contrast, the mesospheric adjustment to stratospheric conditions occurs in just a few days, due to the much shorter timescales associated with gravity-wave propagation and mesospheric radiative

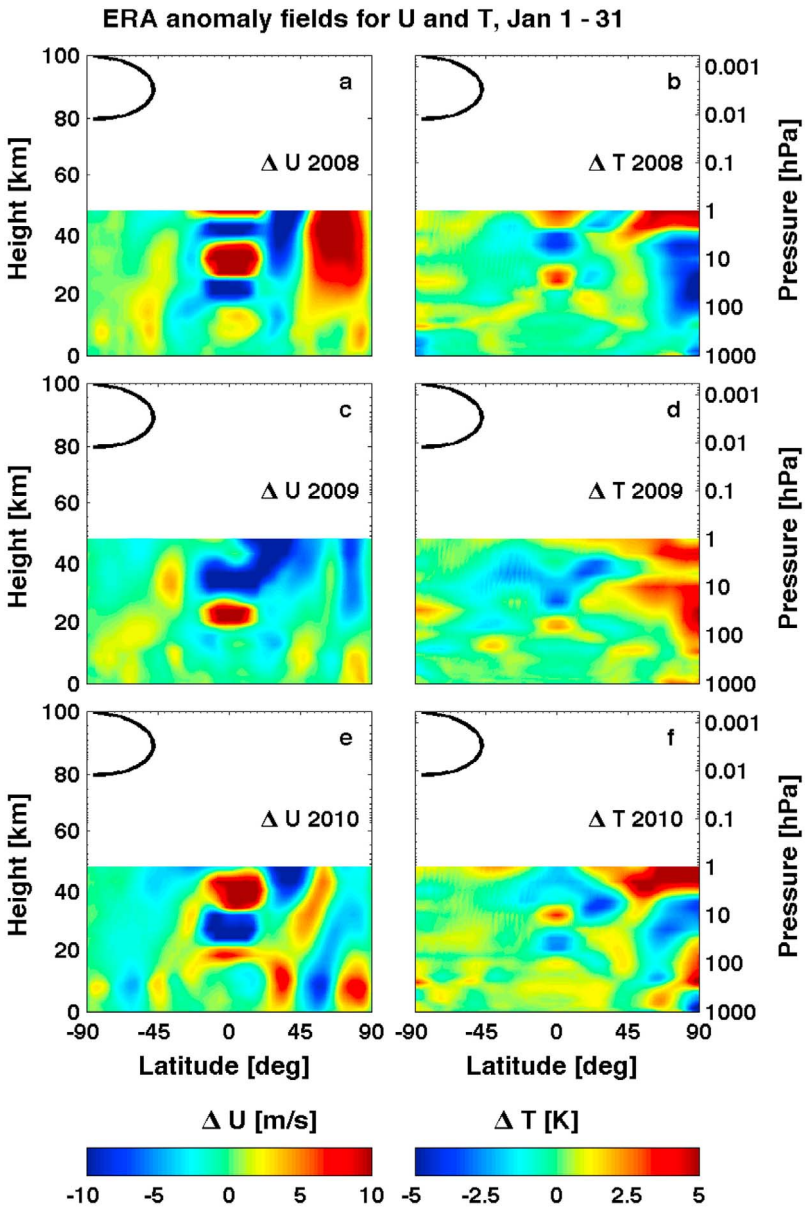

Figure 8. Same as Figure 3, but for the month of January.

forcing. In January, however, which is the peak of the SH PMC season, the variability in the summer stratosphere is generally very small, as can be seen in Figure 8 (same as Figure 3, but for the month of January: ~ day 10 to day 41). This is because stationary planetary waves cannot propagate in the summer zonal flow since they have a westward intrinsic phase speed [*Charney and Drazin*, 1961]. However, PMCs are observed to vary from one year to another in January as well. During this part of the PMC season, the year-to-year variability is to a significant extent controlled by the dynamic activity in the NH winter through inter-hemispheric coupling [*Karlsson et al.*, 2007, 2009a, 2009b].

[27] A natural question to ask is, therefore, whether inter-hemispheric coupling could play a role in PMC onset. The inter-hemispheric coupling signal is such that when the winter zonal wind is strong and the high latitude winter stratosphere is cold, then the summer polar mesopause is anomalously cold, and vice versa [*Karlsson et al.*, 2007, 2009a]. The strongest winter hemisphere anomaly in Figure 3 occurs in 2009, and would imply an anomalously warm summer mesopause, which is not consistent with the PMC observations during the onset period. Thus, we can rule out the winter hemisphere as a significant contributor to the variability in PMC season onset for the years studied here.

[28] **Acknowledgments.** We are grateful to the ECMWF for providing the ERA-Interim Re-analysis; wind and temperature data have been obtained from the ECMWF Data Server. CMAM results were supported by the Canadian Foundation for Climate and Atmospheric Sciences, the Natural Sciences and Engineering Research Council, and the Canadian Space Agency. Funding for the AIM mission was provided by the NASA Small Explorer program under contract NAS5-03132. BK was supported in part by NSF CEDAR grant AGS 0737705.

References

Bailey, S. M., G. E. Thomas, D. W. Rusch, A. W. Merkel, C. D. Jeppesen, J. N. Carstens, C. E. Randall, W. E. McClintock, and J. M. Russell III (2009), Phase functions of polar mesospheric cloud ice as observed by the CIPS instrument on the AIM satellite, *J. Atmos. Sol. Terr. Phys.*, *71*, 373–380, doi:10.1016/j.jastp.2008.09.039.

Becker, E., and G. Schmitz (2003), Climatological effects of orography and land-sea heating contrasts on the gravity-wave driven circulation of the mesosphere, *J. Atmos. Sci.*, *60*, 103–118, doi:10.1175/1520-0469(2003)060<0103:CEOOAL>2.0.CO;2.

Benze, S., C. E. Randall, M. T. DeLand, G. E. Thomas, D. W. Rusch, S. M. Bailey, J. M. Russell III, W. McClintock, A. W. Merkel, and D. Jeppesen (2009), Comparison of polar mesospheric cloud measurements from the cloud imaging and particle size experiment and the solar backscatter ultraviolet instrument in 2007, *J. Atmos. Sol. Terr. Phys.*, *71*, 365–372, doi:10.1016/j.jastp.2008.07.014.

Black, R. X., and B. A. McDaniel (2007), Interannual variability in the Southern Hemisphere circulation organized by stratospheric final warming events, *J. Atmos. Sci.*, *64*, 2968–2974, doi:10.1175/JAS3979.1.

Charney, J. G., and P. G. Drazin (1961), Propagation of planetary-scale disturbances from the lower into the upper atmosphere, *J. Geophys. Res.*, *66*, 83–109, doi:10.1029/JZ066i001p00083.

Chu, X., C. S. Gardner, and R. G. Roble (2003), Lidar studies of interannual, seasonal, and diurnal variations of polar mesospheric clouds at the South Pole, *J. Geophys. Res.*, *108*(D8), 8447, doi:10.1029/2002JD002524.

Dowdy, A. J., R. A. Vincent, M. Tsutsumi, K. Igarashi, Y. Murayama, W. Singer, and D. J. Murphy (2007), Polar mesosphere and lower thermosphere dynamics: 1. Mean wind and gravity wave climatologies, *J. Geophys. Res.*, *112*, D17104, doi:10.1029/2006JD008126.

Fomichev, V. I., W. E. Ward, S. R. Beagley, C. McLandress, J. C. McConnell, N. A. McFarlane, and T. G. Shepherd (2002), Extended Canadian Middle Atmosphere Model: Zonal-mean climatology and physical parameterizations, *J. Geophys. Res.*, *107*(D10), 4087, doi:10.1029/2001JD000479.

Gordley, L. L., et al. (2009), The Solar Occultation for Ice Experiment, *J. Atmos. Sol. Terr. Phys.*, *71*, 300–315, doi:10.1016/j.jastp.2008.07.012.

Gumbel, J., and L. Megner (2009), Charged meteoric smoke as ice nuclei in the mesosphere: Part 1—A review of basic concepts, *J. Atmos. Sol. Terr. Phys.*, *71*, 1225–1235, doi:10.1016/j.jastp.2009.04.012.

Hervig, M., R. E. Thompson, M. McHugh, L. L. Gordley, J. M. Russell III, and M. E. Summers (2001), First confirmation that water ice is the primary component of polar mesospheric clouds, *Geophys. Res. Lett.*, *28*, 971–974, doi:10.1029/2000GL012104.

Hervig, M. E., M. H. Stevens, L. L. Gordley, L. E. Deaver, J. M. Russell III, and S. M. Bailey (2009), Relationships between polar mesospheric clouds, temperature, and water vapor from Solar Occultation for Ice Experiment (SOFIE) observations, *J. Geophys. Res.*, *114*, D20203, doi:10.1029/2009JD012302.

Hines, C. O. (1997a), Doppler-spread parameterization of gravity-wave momentum deposition in the middle atmosphere. Part 1: Basic formulation, *J. Atmos. Sol. Terr. Phys.*, *59*, 371–386, doi:10.1016/S1364-6826(96)00079-X.

Hines, C. O. (1997b), Doppler-spread parameterization of gravity-wave momentum deposition in the middle atmosphere. Part 2: Broad and quasi-monochromatic spectra, and implementation, *J. Atmos. Sol. Terr. Phys.*, *59*, 387–400, doi:10.1016/S1364-6826(96)00080-6.

Holton, J. R. (1983), The influence of gravity wave breaking on the general circulation of the middle atmosphere, *J. Atmos. Sci.*, *40*, 2497–2507, doi:10.1175/1520-0469(1983)040<2497:TIOGWB>2.0.CO;2.

Karlsson, B., H. Körnich, and J. Gumbel (2007), Evidence for interhemispheric stratosphere-mesosphere coupling derived from noctilucent cloud properties, *Geophys. Res. Lett.*, *34*, L16806, doi:10.1029/2007GL030282.

Karlsson, B., C. McLandress, and T. G. Shepherd (2009a), Inter-hemispheric mesospheric coupling in a comprehensive middle atmosphere model, *J. Atmos. Sol. Terr. Phys.*, *71*, 518–530, doi:10.1016/j.jastp.2008.08.006.

Karlsson, B., C. E. Randall, S. Benze, M. Mills, V. L. Harvey, S. M. Bailey, and J. M. Russell (2009b), Intra-seasonal variability of polar mesospheric clouds due to inter-hemispheric coupling, *Geophys. Res. Lett.*, *36*, L20802, doi:10.1029/2009GL040348.

Langematz, U., and M. Kunze (2008), Dynamical changes in the Arctic and Antarctic stratosphere during spring, in *Climate Variability and Extremes During the Past 100 Years*, edited by S. Brönnimann et al., *Adv. Global Change Res.*, *33*, 293–301, doi:10.1007/978-1-4020-6766-2_20.

Lindzen, R. S. (1981), Turbulence and stress owing to gravity wave and tidal breakdown, *J. Geophys. Res.*, *86*, 9707–9714, doi:10.1029/JC086iC10p09707.

Lübken, F.-J. (1999), Thermal structure of the Arctic summer mesosphere, *J. Geophys. Res.*, *104*, 9135–9149.

McClintock, W. E., D. W. Rusch, G. E. Thomas, A. W. Merkel, M. R. Lankton, V. A. Drake, S. M. Bailey, and J. M. Russell III (2009), The cloud imaging and particle size experiment on the Aeronomy of Ice in the Mesosphere mission: Instrument concept, design, calibration, and on-orbit performance, *J. Atmos. Sol. Terr. Phys.*, *71*, 340–355, doi:10.1016/j.jastp.2008.10.011.

McLandress, C. (1998), On the importance of gravity waves in the middle atmosphere and their parameterization in general circulation models, *J. Atmos. Sol. Terr. Phys.*, *60*, 1357–1383, doi:10.1016/S1364-6826(98)00061-3.

McLandress, C., W. E. Ward, V. I. Fomichev, K. Semeniuk, S. R. Beagley, N. A. McFarlane, and T. G. Shepherd (2006), Large-scale dynamics of the mesosphere and lower thermosphere: An analysis using the extended Canadian Middle Atmosphere Model, *J. Geophys. Res.*, *111*, D17111, doi:10.1029/2005JD006776.

Murray, B. J., and E. J. Jensen (2010), Homogeneous nucleation of amorphous solid water particles in the upper mesosphere, *J. Atmos. Sol. Terr. Phys.*, *72*, 51–61, doi:10.1016/j.jastp.2009.10.007.

Rapp, M., and G. E. Thomas (2006), Modeling the microphysics of mesospheric ice particles: Assessment of current capabilities and basic sensitivities, *J. Atmos. Sol. Terr. Phys.*, *68*, 715–744, doi:10.1016/j.jastp.2005.10.015.

Rusch, D. W., G. E. Thomas, W. McClintock, A. W. Merkel, S. M. Bailey, J. M. Russell III, C. E. Randall, C. D. Jeppesen, and M. Callan (2009), The cloud imaging and particle size experiment on the Aeronomy of Ice in the Mesosphere mission: Cloud morphology for the northern 2007 season, *J. Atmos. Sol. Terr. Phys.*, *71*, 356–364, doi:10.1016/j.jastp.2008.11.005.

Russell, J. M., III, et al. (2009), The Aeronomy of Ice in the Mesosphere (AIM) mission: Overview and early science results, *J. Atmos. Sol. Terr. Phys.*, *71*, 289–299, doi:10.1016/j.jastp.2008.08.011.

Shepherd, T. G. (2000), The middle atmosphere, *J. Atmos. Sol. Terr. Phys.*, *62*, 1587–1601, doi:10.1016/S1364-6826(00)00114-0.

Simmons, A., S. Uppala, D. Dee, and S. Kobayashi (2007), ERA-Interim: New ECMWF reanalysis products from 1989 onwards, *ECMWF Newsl. 110*, pp. 25–35, Eur. Cent. for Medium-Range Weather Forecasts, Reading, U. K.

Siskind, D. E., S. D. Eckermann, J. P. McCormack, M. J. Alexander, and J. T. Bacmeister (2003), Hemispheric differences in the temperature of the summertime stratosphere and mesosphere, *J. Geophys. Res.*, *108*(D2), 4051, doi:10.1029/2002JD002095.

Waugh, D. W., W. J. Randel, S. Pawson, P. A. Newman, and E. R. Nash (1999), Persistence of the lower stratospheric polar vortices, *J. Geophys. Res.*, *104*, 27,191–27,201, doi:10.1029/1999JD900795.

S. M. Bailey, Bradley Department of Electrical and Computer Engineering, Virginia Polytechnic Institute and State University, Blacksburg, VA 24061, USA.

V. L. Harvey, B. Karlsson, and C. E. Randall, Laboratory for Atmospheric and Space Physics, University of Colorado at Boulder, Boulder, CO 80309-0392, USA. (bodil.karlsson@lasp.colorado.edu)

M. Hervig, GATS, Inc., Driggs, ID 83422, USA.

J. Lumpe and K. Nielsen, Computational Physics, Inc., Boulder, CO 80301, USA.

J. M. Russell III, Center for Atmospheric Sciences, Hampton University, Hampton, VA 23668, USA.

T. G. Shepherd, Department of Physics, University of Toronto, Toronto, ON M5S 1A7, Canada.